GEOPHYSICAL RESEARCH LETTERS, VOL. 35, L19605, doi:10.1029/2008GL035008, 2008

What do deep sea pressure fluctuations tell about short surface waves?

W. E. Farrell[1] and Walter Munk[2]

Received 12 June 2008; revised 11 August 2008; accepted 15 August 2008; published 9 October 2008.

[1] Short waves centered at the gravity to capillary transition (13.5 Hz) dominate the slope statistics of the sea surface and are responsible for most of the air-sea momentum transfer (wind stress). Little is known about short "gravities." In contrast, long gravities, with their characteristic κ^{-4} spectrum, have extensive observational support. We propose a fundamental distinction between long gravities, with their saturated (wind-independent) spectrum, and short gravities, with their wind-dependent spectrum. Evidence comes (surprisingly) from sea-floor pressure fluctuations associated with non-linear interactions between oppositely traveling surface waves of half their frequency. The bottom pressure spectrum shows a transition at about 6 Hz (3 Hz surface wave frequency) from an f^{-7} to an f^{-3} dependence that we associate with the long to short surface gravity wave transition. Further, the requirement of oppositely traveling energy places an integral restraint on the directional spread of the surface waves. **Citation:** Farrell, W. E., and W. Munk (2008), What do deep sea pressure fluctuations tell about short surface waves?, *Geophys. Res. Lett.*, *35*, L19605, doi:10.1029/2008GL035008.

1. Introduction

[2] Microseismic "noise" at frequencies of order 0.2 Hz has long been attributed to deep sea pressure fluctuations associated with long gravity waves (wave length λ of order 100 m) at the sea surface. Pressure fluctuations at twice the surface wave frequency are excited by wave-wave interaction [*Longuet-Higgins*, 1950; *Cox et al.*, 1984; *Cox and Jacobs*, 1989; *Herbers and Guza*, 1991, 1994]. *Webb and Cox* [1986] extended the range of this effect to 2 Hz acoustic (λ of order 1 m). We propose a further extension to the gravity-capillary (gc) transition, which occurs at wave frequency 13.5 Hz (λ = 1.7 cm), and acoustic frequency 27 Hz. This has interesting implications for the frequency/wave number spectrum of short gravity waves.

2. Deep Sea Pressure Measurements

[3] There is a paucity of VLF observations of pressure in the deep sea obtained with low-noise instrumentation of appropriate bandwidth. The best available data set appears to be the spectra derived by *McCreery et al.* [1993] from an exhaustive analysis of a year's worth of measurements from many hydrophones of the Wake Island Array (WIA). We consider data from WIA hydrophone 74, a bottomed hydrophone in 5500 m of water.

[4] The green circles and triangles in Figure 1 show the average spectrum for WIA 74, under the condition that the wind speed, U, fell in the range $8.94 < U < 10.73$ m/s and $12.52 < U < 14.3$ m/s, respectively. These data were derived from McCreery et al.'s Figure 11 after applying the factor $2\pi f^6$ to unwrap the normalization and to obtain a 1 Hz bandwidth. Substantially the same data, for the lower wind speed, result from digitizing McCreery et al.'s Figure 7 for the WIA 74 median spectrum. For wind speed $U < 9$ m/s and $f > 6$ Hz, the pressure signal fell below the instrument noise floor at this station.

[5] In this paper we attempt to interpret the five right-most green data pairs along the red curve labeled f^{-3} on the left and $f^{7/3}$ on the right.

3. "Long" Surface Waves

[6] There is an extensive literature, mostly going back to the *Phillips* [1958] wave number spectrum

$$\mathrm{F}_\zeta(\kappa) = \tfrac{1}{2}\beta\kappa^{-4}\mathrm{H}(\kappa,\theta)\mathrm{m}^4, \quad \int_{-\pi}^{\pi}\mathrm{H}(\kappa,\theta)d\theta = 1, \tag{1}$$

which Phillips wrote down on the basis only of dimensional considerations. The Phillips constant, β, is determined by experiment. For small wave number, the exponent may be smaller, and Phillips later favored a smaller exponent for all wave numbers, but *Banner*'s [1990] results support the quartic dependence. The function H, called the spreading function, contains the directional properties of the wave field. Integrating over all wave number space gives

$$\langle\zeta^2\rangle = \int_{-\infty}^{\infty}\int_{-\infty}^{\infty}\mathrm{F}_\zeta(\boldsymbol{\kappa})d\kappa_1 d\kappa_2 = \int_{\kappa_0}^{\infty}\int_{-\pi}^{\pi}\mathrm{F}_\zeta(\kappa)\kappa d\kappa d\theta$$
$$= \tfrac{1}{4}\beta\kappa_0^{-2}\mathrm{m}^2 \tag{2}$$

for the mean square elevation. The spectrum is saturated; there is no dependence on wind speed. The wind dependence (in its coarsest form) enters through the lower wave number limit, $\kappa_0 = g/U^2$, which is equivalent to requiring that no spectral component have a phase velocity $C_0 = \sqrt{(g/\kappa_0)}$ faster than the wind speed U. Phillips used β = 0.012; a recent summary by *Banner* [1990] suggests that we cannot do much better than use the Phillips formula, with values of β ranging from 0.008 to 0.016.

[7] The Phillips spectrum has an upper limit, say κ_U, but for $\kappa_U \gg \kappa_0$ there here is no appreciable error in taking $\kappa_U = \infty$ for computing mean square elevation. But the associated mean square slope

$$\langle m^2\rangle = \int_{-\infty}^{\infty}\int_{-\infty}^{\infty}\kappa^2\mathrm{F}_\zeta(\boldsymbol{\kappa})d\kappa_1 d\kappa_2$$
$$\simeq \tfrac{1}{2}\,\beta\int_{\kappa_0}^{\kappa_\mathrm{U}}\kappa^{-1}d\kappa = \tfrac{1}{2}\,\beta\ln(\kappa_0/\kappa_\mathrm{U}) \tag{3}$$

[1]Science Applications International Corporation, San Diego, California, USA.

[2]Scripps Institution of Oceanography, University of California, San Diego, La Jolla, California, USA.

0094-8276/08/2008GL035008$05.00

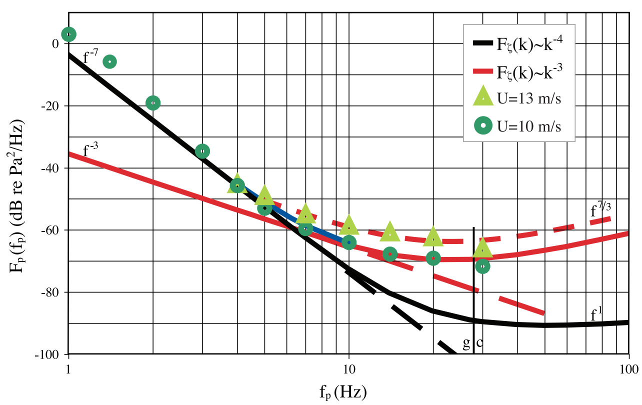

Figure 1. Power spectra of deep ocean pressure fluctuations. Green points are the measured Holu spectrum [*McCreery et al.*, 1993] for 10 m/s (dots) and 13 m/s (triangles) winds. The solid black curve is the computed spectrum inferred from the *Phillips* [1958] long wave κ^{-4} surface wave spectrum. The solid red curve is the computed spectrum inferred from a κ^{-3} surface wave spectrum, and the dotted red curve is the computed spectrum for a 6 dB stronger source. The solid and dotted curves are based on an acoustic radiation theory that allows for surface tension. The dash extensions show the computed spectra when surface tension is ignored.

depends critically on κ_U. The transition in Figure 1 at about f = 6 Hz (κ = 40 radians/meter, henceforth rpm) from the black to the red curve is associated with a transition from the Phillips κ^{-4} spectrum to a spectrum that falls more like κ^{-3}.

4. "Short" Surface Waves

[8] Very little is known about the short gravity waves, which are affected by surface tension at high wave numbers. *Elfouhaily et al.* [1997] and *Hwang* [2005] have provided syntheses of the available information (see Figure 2). To flatten the Phillips spectrum, we have multiplied by κ^{+4} yielding the "uni-directional saturation" version

$$G_s(\kappa) = \tfrac{1}{2}\beta \tag{4}$$

of the Phillips spectrum (horizontal black lines). In particular, we have taken β = 0.008, a value at the low end of Banner's range. The colored curves in Figure 2a show the Elfouhaily et al. and Hwang estimates of $G_S(\kappa)$ for short gravity waves and various wind speeds. Figure 2b shows, along with the Banner spectrum, a family of κ^{-3} models for the short (unsaturated) gravity waves. The models were suggested by the deep pressure data, as shown next.

5. Bottom Pressure Spectrum

[9] *Hughes* [1976] derived an expression for the pressure spectrum caused by opposing surface gravity waves interacting according to the Longuet-Higgins wave-wave mechanism. There have been many derivations of similar formulas (W. E. Farrell et al., Review of acoustic radiation by ocean gravity waves, manuscript in preparation, 2008), but the Hughes formula is unique in that it is based on the wave number spectrum of the surface waves, not the frequency spectrum, and includes the effect of surface tension. Only one other author, *Brekhovskikh* [1966], has included surface tension. This dependence is crucial for modeling pressure in the short gravity wave regime.

[10] The Hughes equation, accounting for a small error later identified (see Farrell et al., manuscript in preparation, 2008), is

$$F_P(\omega_P) = \frac{\pi}{8}\left(\frac{\rho}{c}\right)^2 \omega_P^6 \left\{ \frac{\kappa F_\zeta^2(\kappa_\zeta)}{\partial\omega_\zeta/\partial\kappa} I \right\}, \qquad I = \int H(\theta)H(\theta+\pi)d\theta \tag{5}$$

[11] In equation (5), ρ = 1000 is the mean density of sea water and c = 1500 its mean sound speed. $F_P(\omega_P)$ denotes the pressure spectrum at acoustic frequency ω_P, $F_\zeta(\omega_\zeta)$ the elevation spectrum of gravity waves at frequency $\omega_\zeta = \tfrac{1}{2}\,\omega_P$, and I is the "spreading integral" (see below). The term in curly braces is called the source term.

[12] In the long gravity wave limit, (5) reduces to the more familiar expression [*Kibblewhite and Wu*, 1996, equation 4.107]

$$F_p(\omega_p) = \frac{\pi}{2}\left(\frac{\rho g}{c}\right)^2 \omega_p^3 \{F_\zeta^2(\omega_\zeta) I\} \tag{6}$$

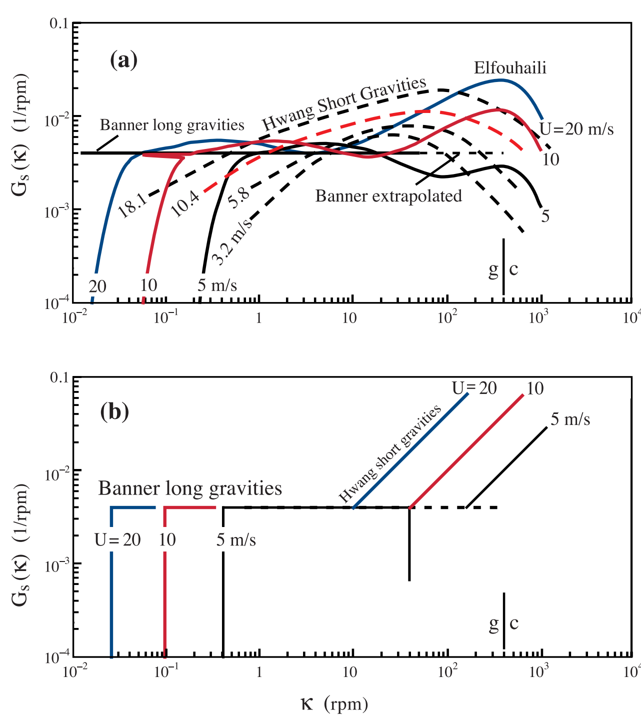

Figure 2. The saturation spectrum $G_s(\kappa)$. (a) The Banner spectrum for long gravity waves is extended to the Banner limit of 31 rpm. The *Elfouhaily et al.* [1997] spectra (solid curves) are peaked at the gc transition. *Hwang* [2005] spectra (dashed) are peaked in the short gravity wave band. (b) Idealized representation of the saturation spectrum. The transition from the Banner-like white spectrum with low-frequency wind cut-offs to the Hwang spectra is not clear.

Table 1. Properties of Long and Short Surface Gravity Wave Models and the Double-Frequency Pressure Models That Are Excited by the Wave-Wave Interaction Mechanism[a]

	Long Gravity Waves	Short Gravity Waves
Dispersion relation	$\omega^2 = g\kappa$	$\omega^2 = g\kappa(1 + (\kappa/\kappa_{gc})^2)$ $\kappa_{gc} = \sqrt{(g/\gamma)} = 374$ rpm
Wave models	$F_\zeta(\kappa) = \frac{1}{2}\beta\kappa^{-4}$ m^4 $F_\zeta(\omega_\zeta) = \beta g^2\omega^{-5}$ m^2/(rad/sec)	$F_\zeta(\kappa) = \gamma\kappa^{-3}$ m^4 $F_\zeta(\omega_\zeta)$, not a single power of ω
Wave number and frequency limits	$\kappa_{max} = 40$ rpm $\omega_{max} = 20$ rad/sec $f_{max} = 3.15$ Hz	$\kappa_{min} = 40$ rpm, $\kappa_{max} = \kappa_{gc}$ $\omega_{min} = 20$, $\omega_{max} = 85$ rad/sec $f_{min} = 3.15$, $f_{max} = 13.6$ Hz
Pressure frequency limits	$\omega_P = 2\ \omega_\zeta$ $f_{Pmax} = 6.3$ Hz, $U = 10$ $f_{Pmax} = 4.5$ Hz, $U = 13$	$\omega_P = 2\ \omega_\zeta$ $f_{Pmin} = 6.3$ Hz, $f_{Pmax} = 27$ Hz
Pressure source model	$\frac{1}{2}\beta^2 g^6 \omega_\zeta^{\ -13}\ I_L$	$\frac{2\gamma^2\omega_\zeta\kappa^{-5}}{g\left(1+\left(\kappa/\kappa_{gc}\right)^2\right)} I_S$ $\approx 2\ \gamma^2 g^4 \omega_\zeta^{-9}\ I_S$, $\kappa \ll \kappa_{gc}$
Pressure spectrum model	$F_P(\omega_P) = A\omega^{-7}\beta^2\ I_L$ Pa^2/(rad/sec) $A = 6.3 \times 10^8\ (512\pi(\rho g^3/c)^2)$ $\beta^2\ I_L = 3.8 \times 10^{-5}$	F_P is not a simple power law, but $F_P(\omega_P) = (A/(2g)^2)\omega^{-3}\gamma^2\ I_S$, $\kappa \ll \kappa_{gc}$ $\gamma^2\ I_s = 5.7 \times 10^{-9}$ $\gamma = \beta/80$, if $I_s = I_L$

[a]The pressure source model is the source term of equation (5), evaluated for the dispersion relation and defined wave models.

[13] Most of the acoustic pressure is caused by wave motion nearly overhead. *Cato* [1991] showed that the energy that propagates to the far field can be represented as a surface distribution of random, vertically-oriented dipoles. Consider a disk of radius r_{max} centered over the pressure measurement point at depth d. Then the fractional contribution to the power at d from surface waves within the disk is given by

$$\frac{F_P(r < r_{max})}{F_P(r < \infty)} = \frac{1}{1 + (d/r_{max})^2} \tag{7}$$

[14] Thus, for a bottomed hydrophone, half the power comes from surface waves within one water-depth of the overhead point, 90% from surface waves within three water-depths. In applying equation (5) we assume that the conditions for the second-order pressure generation are satisfied.

[15] Turning back to Figure 1, the black curve shows the computed pressure spectrum $F_P(\omega_P)$ in response to an f^{-5} (κ^{-4}) Phillips surface wave spectrum. The details behind the pressure computation are provided in Table 1. In particular, as seen in the last row, the black straight line, and its dash extension, correspond to a value of $\beta^2 I_L$ (the only free parameter) given by $\beta^2 I_L = 3.8 \times 10^{-5}$.

[16] Imagine that the Phillips 58 spectrum extends indefinitely to higher frequencies. The black curve would then continue indefinitely along an f^{-7} slope, provided surface tension was neglected (black dashed, equation (6)). When surface tension is taken into account, the computed pressure spectrum above 10 Hz curves upwards from the linear extension (equation (5)). Similarly, the red curve (see Table 1) designates the pressure spectrum for an f^{-3} (κ^{-3}) surface wave spectrum, with the red dashed curve corresponding to a gravity-only ocean.

[17] Starting from the left, the measured pressure spectrum (green circles) follows a straight black f^{-7} line, which is the appropriate slope for the f^{-5} Phillips 58 surface wave spectrum. If the Phillips 58 spectrum were to extend to the gc transition at 29 Hz, the computed pressure spectrum would start deviating from the straight f^{-7} line, curving upwards above 10 Hz. In fact, the deviation occurs at 6 Hz (3 Hz and 5.6 cycles/meter surface wave frequencies) and is not the response to surface tension, but the result of a transition of the surface wave spectrum from a Phillips 58 f^{-5} dependence to something like an f^{-3} dependence. This important transition from long to short gravity waves is roughly consistent with surface measurements by *Elfouhaily et al.* [1997] and *Hwang* [2005].

[18] We notice also that the black curve is consistent with both 10 and 13 m/s winds, whereas distinct red curves, separated by 6 dB, need to be drawn for the two wind speeds. Accordingly the transition marks the change from a saturated long wave spectrum to an unsaturated short wave spectrum.

6. Source Term and Spreading Integral

[19] The spreading integral [*Wilson et al.*, 2003], introduced in (5), expresses the extent to which there are opposing wave numbers in the spectrum. It involves H, the spreading function introduced in equation (1). The spreading function is a fundamental property of the surface wave spectrum. There is a large theoretical and experimental literature on the spreading function for long gravity waves. Very little is known about the spreading function for short gravity waves [*Munk*, 2008].

[20] *Webb and Cox* [1986] have demonstrated that plausible estimates of the spreading integral could be inferred from deep ocean pressure data. *Wilson et al.* [2003] followed a different strategy, using deep sea pressure data in the band between 0.1 and 1 Hz to confirm a spreading integral calculated from surface measurements. It is implicit in (5) and (6) that the interacting waves are exactly opposite in direction and equal in frequency. *Herbers and Guza* [1994] show calculations of the spreading integral (called, by them, *M*) under more general interactions, but their results only apply at lower frequencies.

[21] A visual alignment of the black curve and the green points for frequencies less than 7 Hz yields the factor $\beta^2 I_L = 3.8 \times 10^{-5}$, where we use I_L to indicate the spreading

integral of long gravity waves. The spectral amplitude of the wave field and the spreading integral cannot be separately evaluated from these data alone. However, since the spreading integral can never exceed $1/(2\pi)$, we can place a lower bound on the Phillips constant,

$$\beta \geq \sqrt{2\pi 3.8 \times 10^{-5}} = 1.5 \times 10^{-2} \tag{8}$$

[22] The lower bound given by (8) is near the upper limit of the range Banner considered. However, in view of the cautions expressed by *McCreery et al.* [1993] over calibration accuracy, we emphasize our method of analysis rather than this particular result. Furthermore, bottom interaction, which may raise the acoustic pressure several dB and cause a proportional over-estimate of $\beta^2 \mathrm{I_L}$, has been neglected.

[23] A qualitative fit to the five green dots (U = 10) with $f > 5$ Hz is obtained with a short gravity wave model that intersects the long gravity wave model at an acoustic frequency of 6.3 Hz. At this frequency the acoustic source functions are equal, and using the formulas in Table 1, we infer that

$$\gamma^2 \mathrm{I_S} = \left(\frac{g}{2\omega_\zeta^2}\right)^2 \beta^2 \mathrm{I_L} = 1.5 \times 10^{-4} \beta^2 \mathrm{I_L} \tag{9}$$

[24] Alternatively, noting that the frequency where the pressure models intersect, 6.3 Hz, corresponds to the wave number, 40 rpm, where the wave models intersect, we immediately see that $\gamma = \beta/80$, which is the same as (9) in the case where the spreading integrals are identical.

[25] From (9), and the value of $\beta^2 \mathrm{I_L}$, the following bounds are obtained for γ,

$$\begin{aligned} \gamma(10) &\geq \sqrt{2\pi 5.7 \times 10^{-9}} = 1.9 \times 10^{-4} \\ \gamma(13) &\geq 4.0 \times 10^{-4} \end{aligned} \tag{10}$$

[26] The spreading integral can range from 0 (no azimuthal overlap) to $1/(2\pi)$ (equal energy in all directions). As shown above, deep sea measurements provide an integral constraint on $\mathrm{H}(\theta)$ through (5). But the accuracy with which the spreading integral can be estimated is constrained by its linkage to the wave Phillips constant, which appears quadratically in the pressure formula.

7. Conclusions

[27] Interpreting the pressure fluctuations by the standard acoustic radiation theory provides evidence for a transition near 6 Hz (3 Hz, 6 cycle/meter surface waves) from long to short gravity waves. The transition frequency decreases as the wind speed increases. The long wave spectrum is saturated, the short wave spectrum is not saturated. The pressure measurements confirm the ω^{-5} (or κ^{-4}) long surface wave spectrum (as has long been known), and suggest an ω^{-3} (or κ^{-3}) short surface wave spectrum. Further, the requirement of oppositely traveling wave energy places an integral restraint on the directional spread of the surface waves. The inferred wave spectrum is not inconsistent with the *Elfouhaily et al.* [1997] and *Hwang* [2005] wave models developed by direct surface observations.

[28] **Acknowledgments.** W. E. Farrell was supported primarily by Science Applications International Corporation with supplementary funding provided by the Office of Naval Research. Walter Munk has the Secretary of the Navy Chair in Oceanography.

References

Banner, M. L. (1990), Equilibrium spectra of wind waves, *J. Phys. Ocean.*, *20*, 966–984.
Brekhovskikh, L. M. (1966), Underwater sound waves generated by surface waves in the ocean, *Izv. Atmos. Oceanic Phys.*, *2*, 970–980.
Cato, D. H. (1991), Theoretical and measured underwater noise from surface wave orbital motion, *J. Acoust. Soc. Am.*, *89*, 1096–1112.
Cox, C. S., and D. C. Jacobs (1989), Cartesian diver observations of double frequency pressure fluctuations in the upper levels of the ocean, *Geophys. R. Lett.*, *16*, 807–810.
Cox, C. S., T. Deaton, and S. Webb (1984), A deep-sea differential pressure gauge, *J. Atmos. Oceanic Technol.*, *1*, 237–246.
Elfouhaily, T., B. Chapron, K. Katsaros, and D. Vandemark (1997), A unified directional spectrum for long and short wind-driven waves, *J. Geophys. Res.*, *102*, 15,781–15,796.
Herbers, T. H. C., and R. T. Guza (1991), Wind-wave nonlinearity observed at the sea floor. Part I: Forced-wave energy, *J. Phys. Oceanogr.*, *21*, 1740–1761.
Herbers, T. H. C., and R. T. Guza (1994), Nonlinear wave interactions and high-frequency seafloor pressure, *J. Geophys. Res.*, *99*, 10,035–10,048.
Hughes, B. (1976), Estimates of underwater sound (and infrasound) produced by nonlinearly interacting ocean waves, *J. Acoust. Soc. Am.*, *60*, 1032–1039.
Hwang, P. A. (2005), Wave number spectrum and mean square slope of intermediate-scale ocean surface waves, *J. Geophys. Res.*, *110*, C10029, doi:10.1029/2005JC003002.
Kibblewhite, A. C., and C. Y. Wu (1996), *Wave Interactions as a Seismo-acoustic Source*, Springer, New York.
Longuet-Higgins, M. S. (1950), A theory of microseisms, *Philos. Trans. R. Soc. London*, *243*, 1–35.
McCreery, C. S., F. K. Duennebier, and G. H. Sutton (1993), Correlation of deep ocean noise (0.4–30 Hz) with wind, and the Holu spectrum-A worldwide constant, *J. Acoust. Soc. Am.*, *93*, 2639–2648.
Munk, W. (2008), An inconvenient sea-truth: Spread, steepness and skewness of surface slopes, *Annu. Rev. Mar. Sci.*, doi:10.1146/annurev.marine.010908.163940, in press.
Phillips, O. M. (1958), The equilibrium range in the spectrum of wind-generated waves, *J. Fluid Mech.*, *4*, 426–434.
Webb, S. C., and C. S. Cox (1986), Observations and modeling of seafloor microseisms, *J. Geophys. Res.*, *91*, 7343–7358.
Wilson, D. K., G. V. Frisk, T. E. Lindstrom, and C. J. Sellers (2003), Measurement and prediction of ultralow frequency ocean ambient noise off the eastern U.S. coast, *J. Acoust. Soc. Am.*, *113*, 3117–3133, doi:10.1121/1.1568941.

W. E. Farrell, Del Mar, CA 92014, USA. (wef@farrell-family.org)
W. Munk, Scripps Institution of Oceanography, University of California, San Diego, 9500 Gilman Drive MC 0225, La Jolla, CA 92093-0225, USA.